

Electronic Supplementary Information

NiFe (sulfur)oxyhydroxide porous nanoclusters/Ni foam composite electrode driving large-current-density oxygen evolution reaction with ultra-low overpotential

Yanqing Wang^a, Yuemeng Li^a, Liping Ding^b, Zhe Chen^a, Aaron Ong^a, Wanheng Lu^a, Tun Seng Herng^a,

Xinwei Li^a, Jun Ding^{a,*}

a Department of Materials Science & Engineering, National University of Singapore, 117575,
Singapore

b School of Chemistry and Chemical Engineering, Nantong University, Nantong 226007, China

Experimental Section

Materials

Ni foam(NF) conductive support was bought from Latech Scientific Supply Pte. Ltd. $\text{NiSO}_4 \cdot 6\text{H}_2\text{O}$, $(\text{NH}_4)_2\text{Fe}(\text{SO}_4)_2 \cdot 6\text{H}_2\text{O}$, $\text{Na}_2\text{S}_2\text{O}_3 \cdot 5\text{H}_2\text{O}$, KOH, H_2SO_4 (95-98wt%) and ethyl alcohol were purchased from Sigma-Aldrich Chemical Reagent Co.

Preparation of (Ni, Fe)SO(OH)/NF composite electrode

(Ni, Fe)SO(OH)/NF composite electrode was fabricated as follows. In a typical synthesis, a piece of NF was dipped into ethyl alcohol at room temperature for 2 min to remove the oil. To remove the oxide of NF surface, then NF was immersed in 5 volume% H_2SO_4 for 2min at room temperature. Finally, NF was dipped into thiosulfate metal solution for 2h at 90°C. Thiosulfate metal solution contains 20g/L $\text{Na}_2\text{S}_2\text{O}_3 \cdot 5\text{H}_2\text{O}$, 3g/L $\text{NiSO}_4 \cdot 6\text{H}_2\text{O}$ and 3g/L $(\text{NH}_4)_2\text{Fe}(\text{SO}_4)_2 \cdot 6\text{H}_2\text{O}$. Notably, NF was cleaned by deionized water for a few times among the above two processes.

Preparation of (Ni, Fe)O(OH)/NF composite electrode

(Ni, Fe)O(OH)/NF composite electrode was fabricated by the same preparation method with (Ni, Fe)SO(OH)/NF composite electrode. The only difference is that the metal solution doesn't contains $\text{Na}_2\text{S}_2\text{O}_3 \cdot 5\text{H}_2\text{O}$.

Characterizations

ZEISS SEM Supra 40 was used to observe the microscopic morphology of samples. Transmission electron microscopy (TEM) of samples was measured on a JEOL-3010 (300 kV acceleration voltage). XRD patterns were carried out by Bruker D8 Advanced Diffractometer System. X-ray photoelectron spectroscopy (XPS, Kratos

AXIS Ultra DLD) was employed to determine the element analysis of samples. ICP (Perkin Elmer Optima 5300DV) test was conducted to detect the element analysis of electrolyte. The conductivity of the coating and the substrate was measured by conductive-atomic force microscopy (c-AFM), where the surface of the coating or the substrate was polarized by a dc voltage and scanned by a conductive c-AFM tip in the contact mode to profile the structure and current over the surface. The c-AFM measurements in this work were conducted on a commercial Scanning Probe Microscopy (SPM) system (MPF-3D, Asylum Research, Oxford Instruments, USA), and conductive Pt-coated Silicon tips with a spring constant of 2 N/m and a tip radius of about 15 nm (AC-240TM, Olympus, Japan) were used. To avoid the tip-induced modification to the sample structure and to ensure a sufficient current sensitivity, a proper set point, corresponding to a contact force of 20 nN, was chosen for c-AFM scanning. The scan rate is 0.5 Hz.

To characterize the electron transfer ability of electrode, three methods including surface current mapping method, point measurement method and two probe method were employed in this work. Firstly, C-AFM was used to detect surface current distribution of different OER catalysts. In this method, c-AFM tip is grounded and varied voltage is applied to the sample surface. The current image shows the current over the sample surface. Point measurement method was used to detect I-V curves of different OER catalysts. In this method, the bottom of sample is grounded and bias is applied to the tip. To confirm the above results of two methods further, two probe method was used to detect the conductivity of catalyst film on Ni plate.

Electrochemical measurements

OER process was investigated in a typical three-electrode cell connected to a Bio-logic VMP 3. In this cell, the (Ni, Fe)SO(OH)/NF, Pt and Hg/HgO were used as the working electrode ($1 \times 1 \text{ cm}^2$), a counter electrode and a reference electrode, respectively. According to $E(\text{RHE}) = E_{\text{Hg/HgO}} + 0.059\text{pH} + 0.098\text{V}$, the measured potentials were all converted to reversible hydrogen electrodes (RHE). LSV curves were measured with the scan rates of 5 mV/s . All the Tafel slopes of the experiments were derived from LSV curves. The chronoamperometric (CA) measurement was usually conducted to confirm long-term OER stability of catalyst for at least 10h. To further confirm much superior long-term OER stability of catalyst, CA test was extended to 50h. SEM test of the catalyst and ICP test of electrolyte after chronoamperometric (CA) measurement were determined to confirm the structural stability of the catalyst. Please note that all the other electrochemical data were shown with 95% IR compensation.

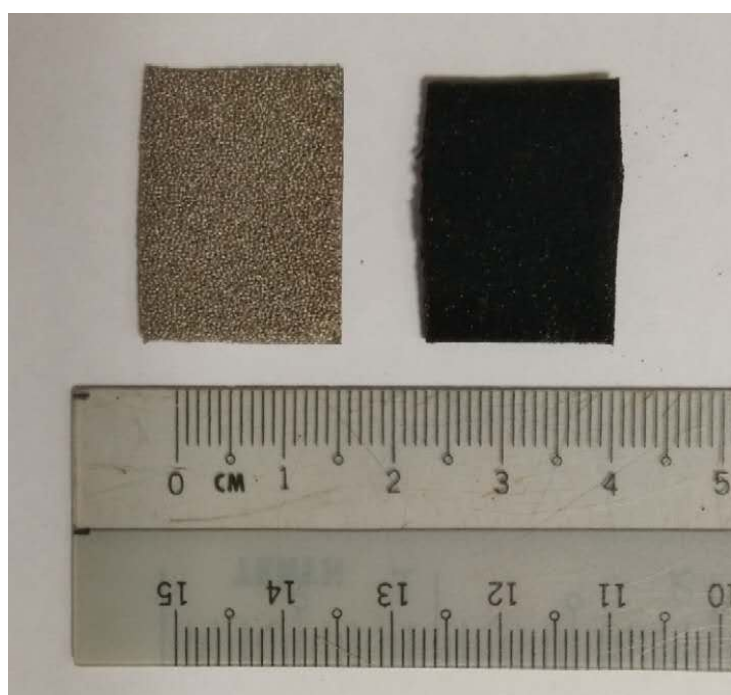


Figure S1 the digital photos of Nickel foam after pretreatment(left) and (Ni, Fe)SO(OH)(right)

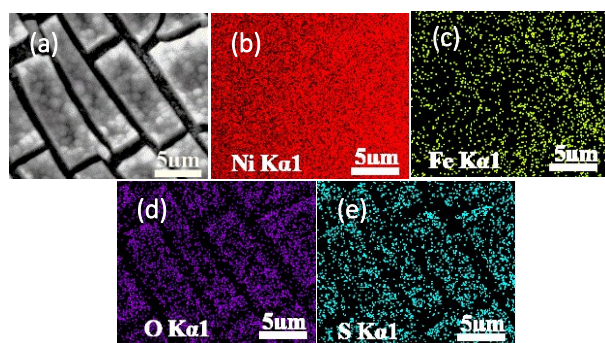


Figure S2 EDS mapping results of (Ni, Fe)SO(OH). (a) EDS Mapping image of (Ni,Fe)SO(OH)

(b-e) EDS mapping images of elements of (Ni,Fe)SO(OH)

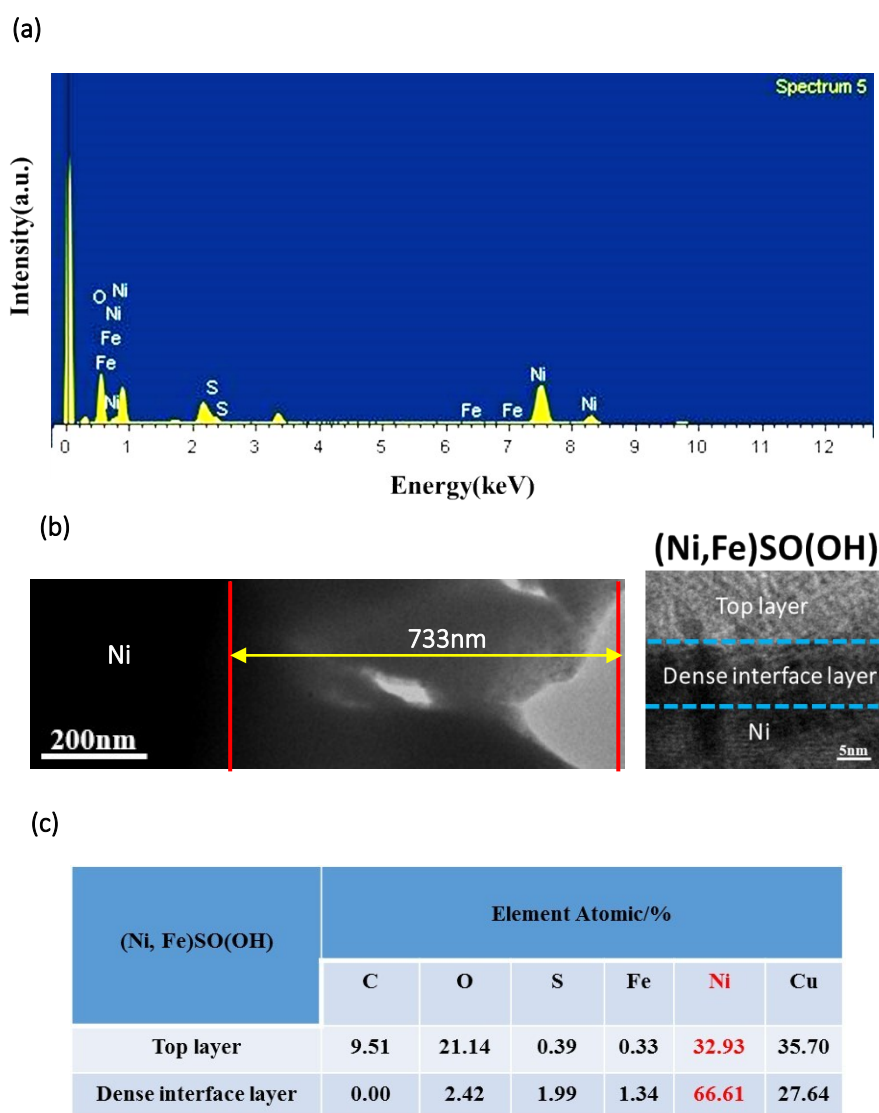
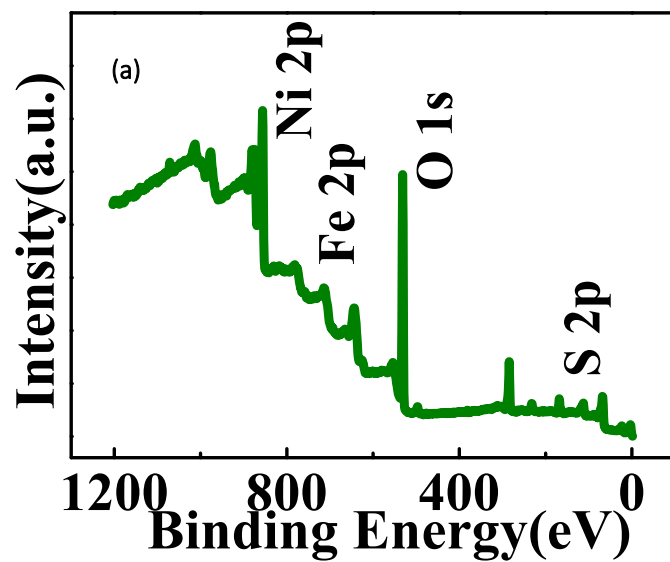


Figure S3 EDS test results and cross section morphology of (Ni, Fe)SO(OH). (a) EDS spectrum of (Ni, Fe)SO(OH). (b) the cross section SEM and TEM images of (Ni, Fe)SO(OH) (c) EDX(TEM attached) results of the top layer and dense interface layer of (Ni, Fe)SO(OH). Note: C element comes from polymer binder which was used for observing the cross section morphology of samples, Cu element comes from TEM holder.



(b)

Element	Atomic/%
Ni	37.17
Fe	11.52
S	4.09
O	47.22
Total	100.00

Figure S4 XPS full spectrum(a) and the surface layer element atomic content(b) of (Ni,

Fe)SO(OH).

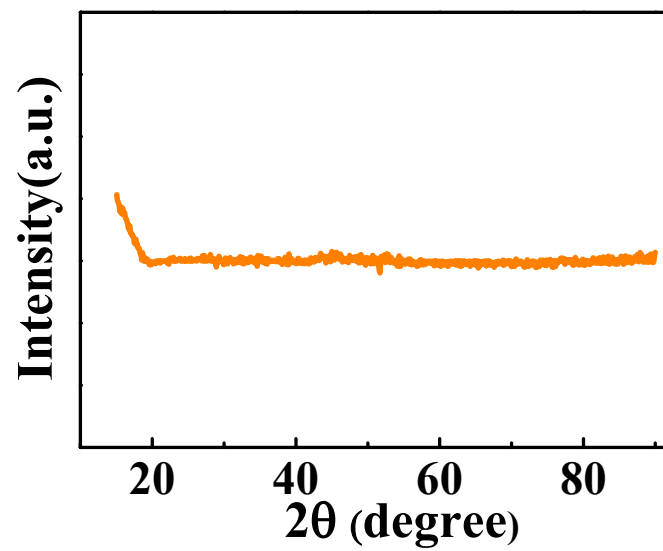


Figure S5 XRD patterns of (Ni, Fe)SO(OH).

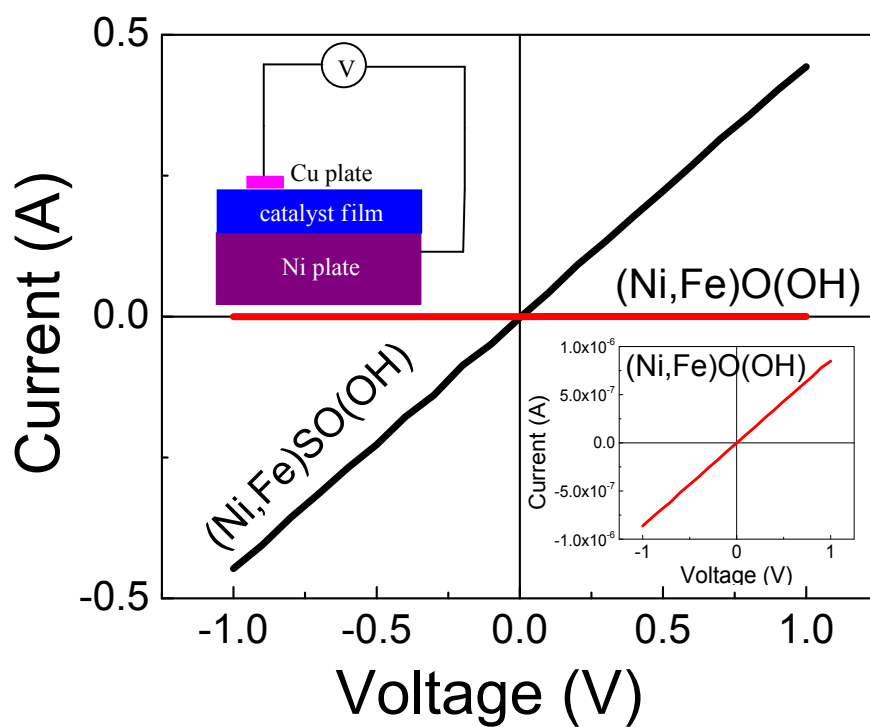


Figure S6 The conductivity results of different catalytic film by two probe method. Insert picture: the test model of two probe method (upper left corner) and magnification curve of (Ni,Fe)O(OH) curve(bottom right corner).

Note: According to the above measurement results, the resistance of (Ni, Fe)SO(OH) and (Ni, Fe)O(OH) is 2.236Ω and $1.162 \times 10^6\Omega$, respectively. Meanwhile, the thickness of the (Ni, Fe)SO(OH) and (Ni, Fe)O(OH) is about $0.730\mu\text{m}$ and $2\mu\text{m}$, respectively. According to the resistivity equals the resistance multiplied by the thickness, so the resistivity of (Ni, Fe)SO(OH) is rough calculated about $1.6 \times 10^{-6} \Omega \cdot \text{m}$, while the resistivity of (Ni, Fe)O(OH) is rough calculated about $2.3 \Omega \cdot \text{m}$.

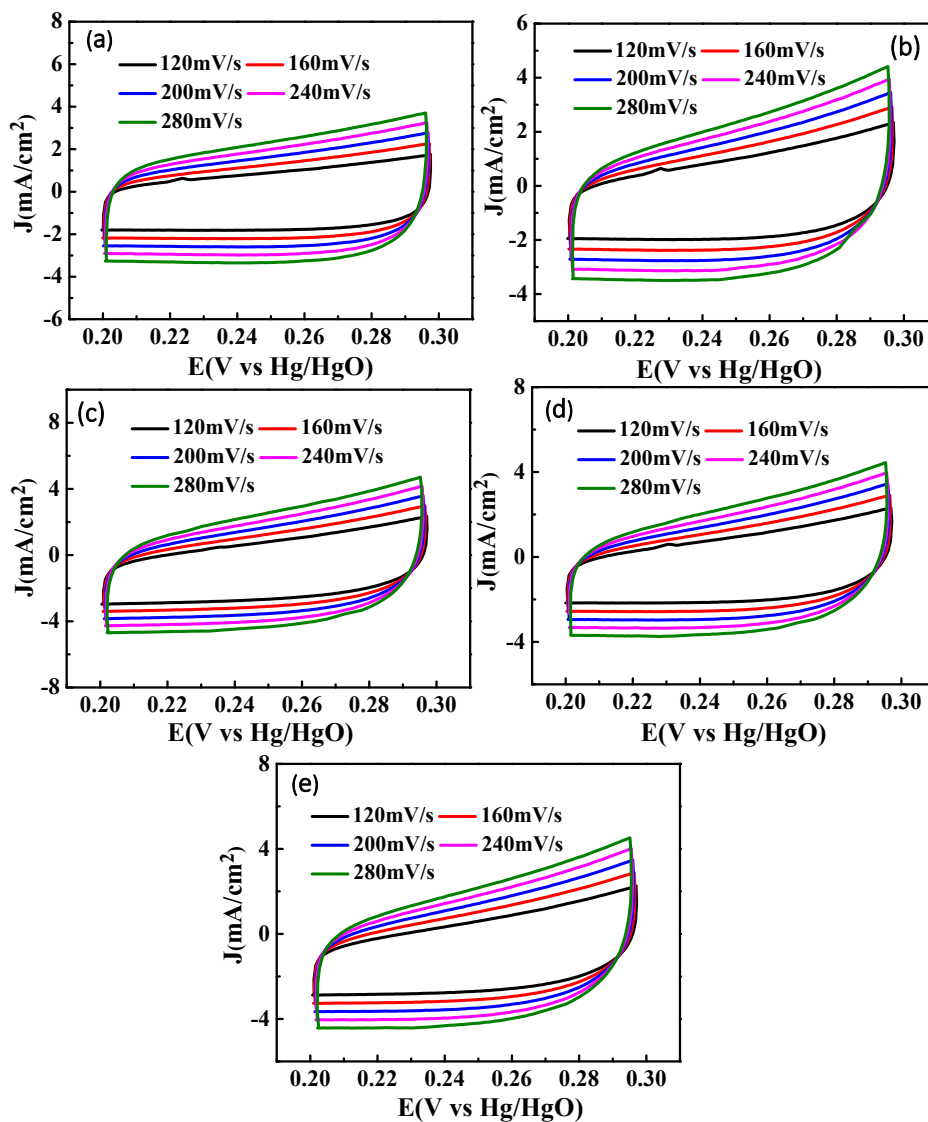


Figure S7 CV curves at different scan rates in the non-Faradaic capacitance current range for (Ni, Fe)SO(OH) under different reaction time (a) 0.5h (b) 1h (c) 2h (d) 4h (e) 8h

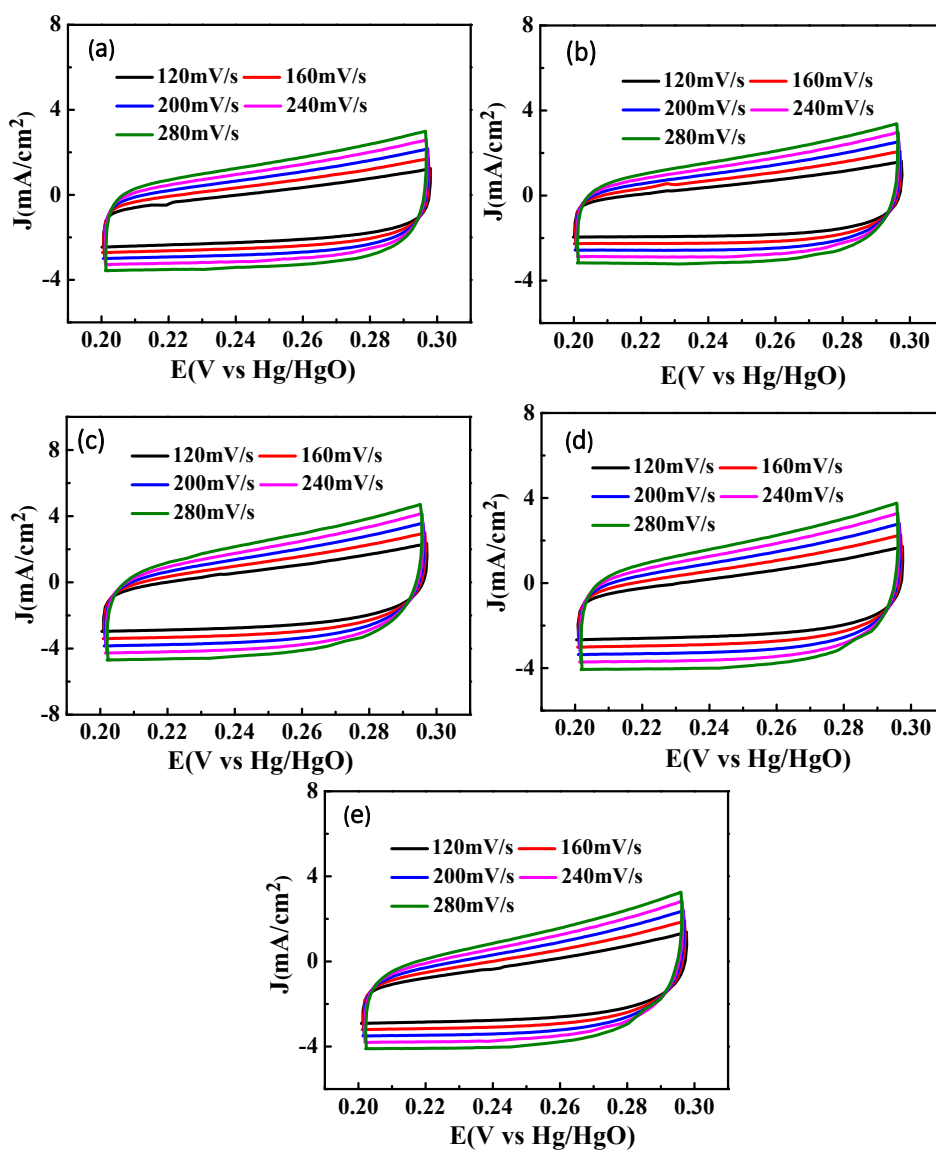


Figure S8 CV curves at different scan rates in the non-Faradaic capacitance current range for (Ni, Fe)SO(OH) under different the mass ratio of Ni salt and Fe salt. (a) 3:1 (b) 2:1 (c) 1:1 (d) 1:2 (e)

1:3

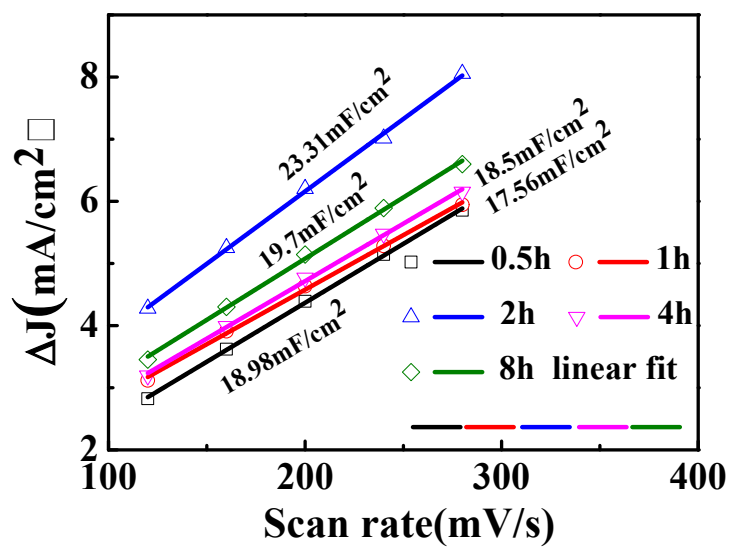


Figure S9 the corresponding capacitive current differences as a function of scan rates at 0.26V vs.

Hg/HgO for (Ni, Fe)SO(OH) under different reaction time

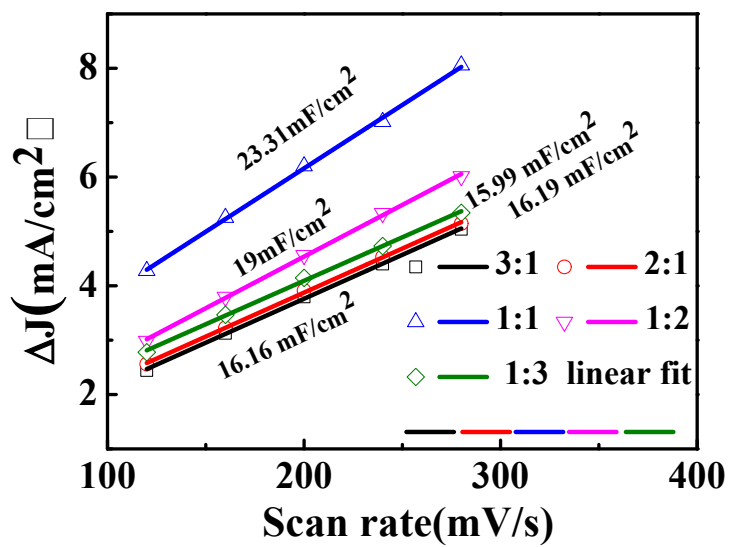


Figure S10 the corresponding capacitive current differences as a function of scan rates at 0.26V vs. Hg/HgO for (Ni, Fe)SO(OH) under different the mass ratio of Ni salt and Fe salt.

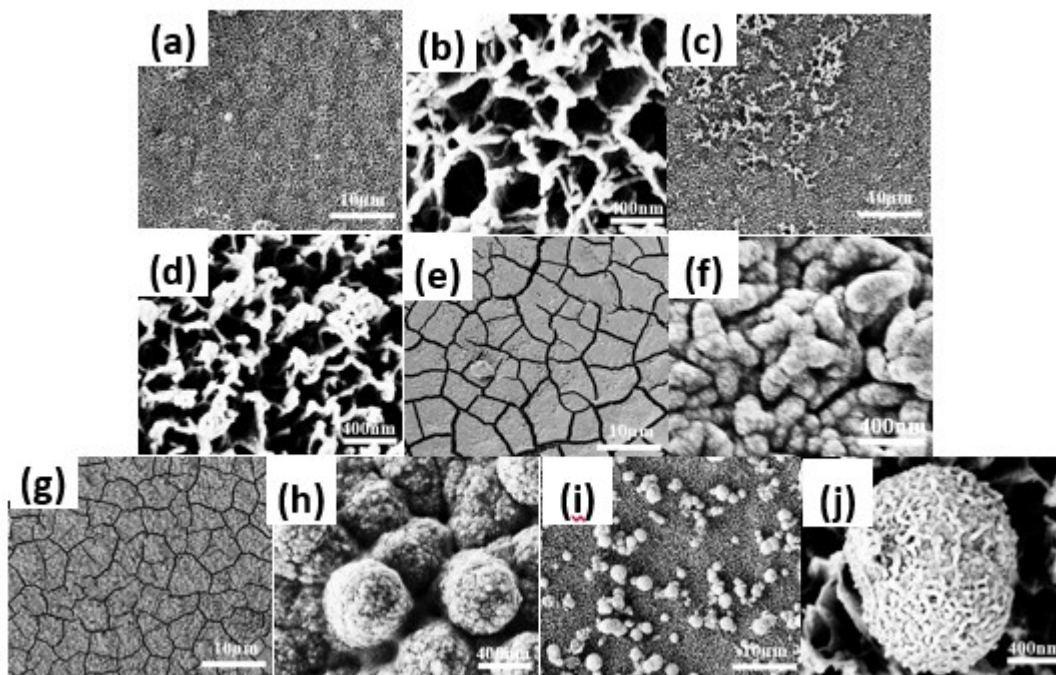


Figure S11 The influence of different reaction time on the morphology of (Ni, Fe)SO(OH) (a~b)

0.5h (c~d) 1h (e~f) 2h (g~h) 4h (i~j) 8h m(Ni salt):m(Fe salt)=1:1.

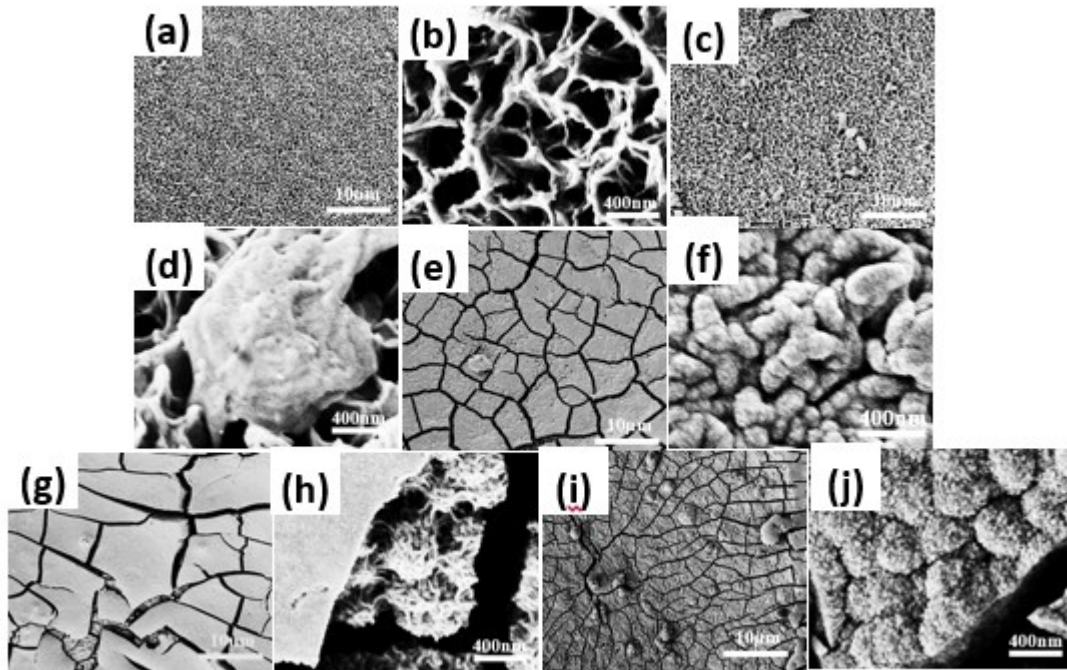


Figure S12 The influence of different m(Ni salt):m(Fe salt) on the morphology of (Ni, Fe)SO(OH)

(a~b) 3:1 (c~d) 2:1 (e~f) 1:1 (g~h) 1:2 (i~j) 1:3 reaction time=2h.

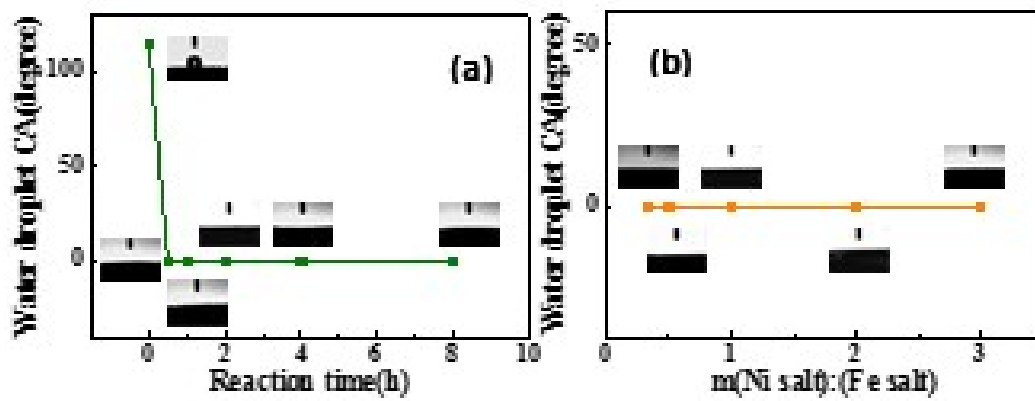


Figure S13 The influence of the reaction time (a) and the ratio of $m(\text{Ni salt})$ and $m(\text{Fe salt})$ (b) on the hydrophilicity of $(\text{Ni,Fe})\text{SO}(\text{OH})/\text{NF}$ electrode

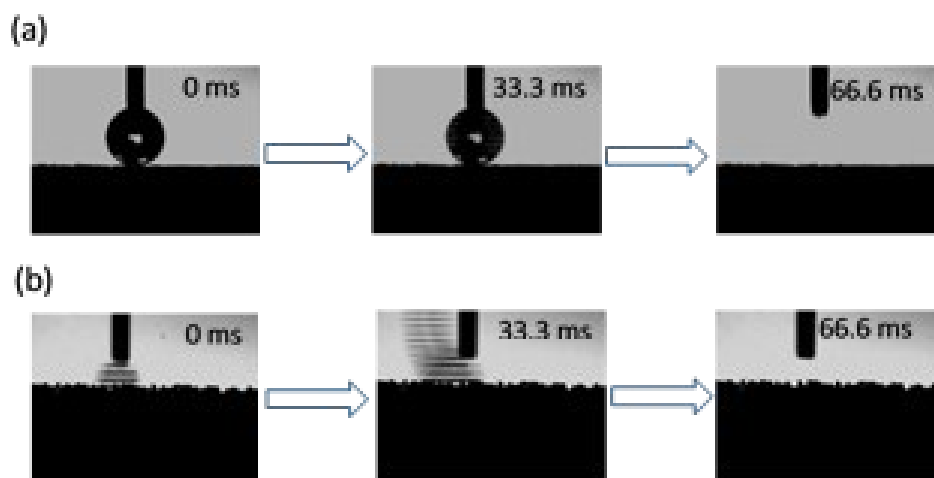


Figure S14 The water droplet wetting process (a) and the air bubble underwater wetting process(b)

observation of (Ni,Fe)SO(OH)/NF electrode.

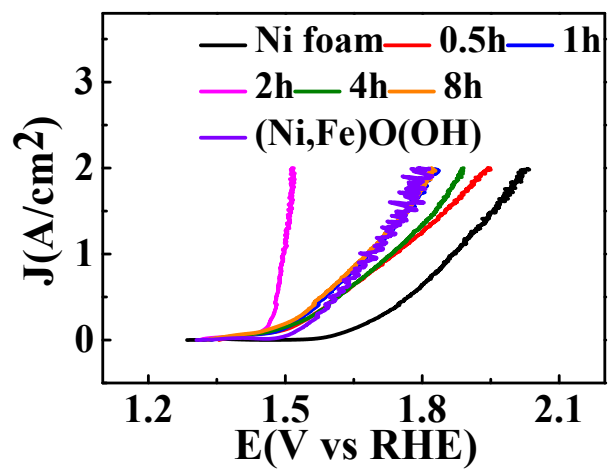


Figure S15 the influence of the reaction time on the LSV performance of (Ni,Fe)SO(OH)/NF

electrode

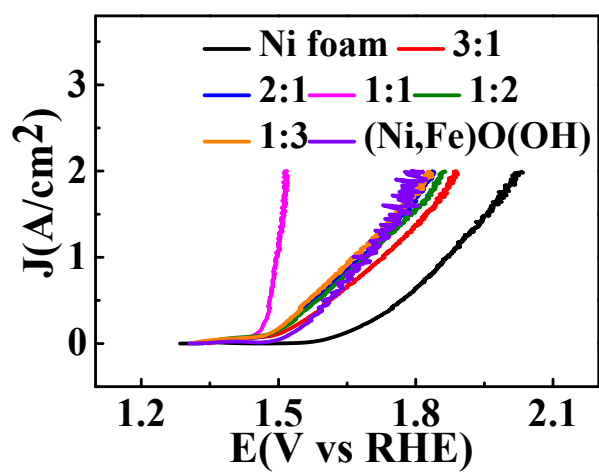


Figure S16 the influence of the ratio of m(Ni salt) and m(Fe salt) on the LSV performance of (Ni,Fe)SO(OH)/NF electrode

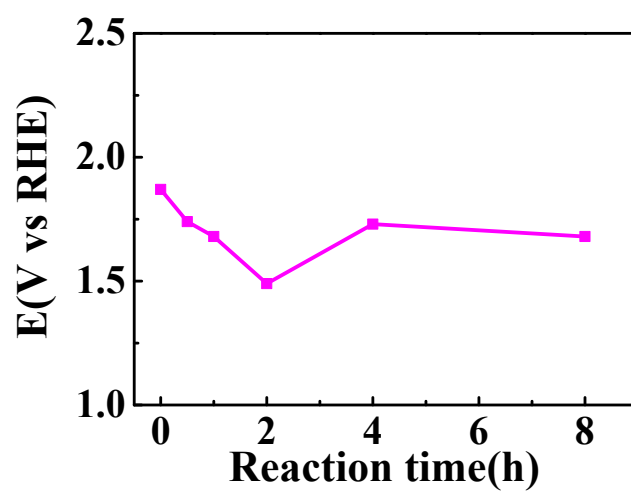


Figure S17 the influence of the reaction time on the potential value at $1\text{A}/\text{cm}^2$ of

(Ni,Fe)SO(OH)/NF electrode

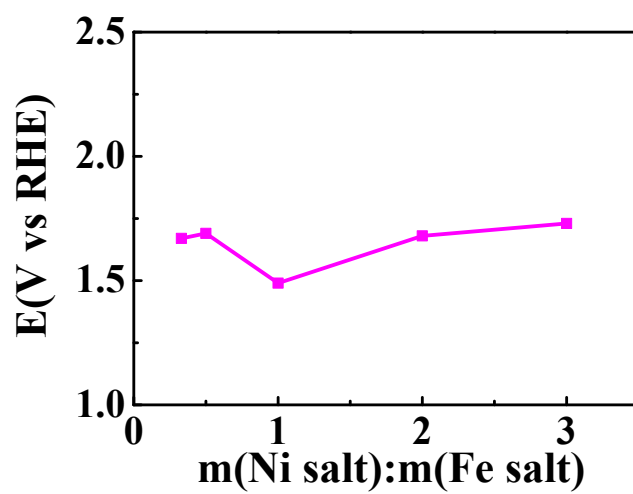


Figure S18 the influence of the ratio of m(Ni salt) and m(Fe salt) on the potential value at $1\text{A}/\text{cm}^2$ of (Ni,Fe)SO(OH)/NF electrode

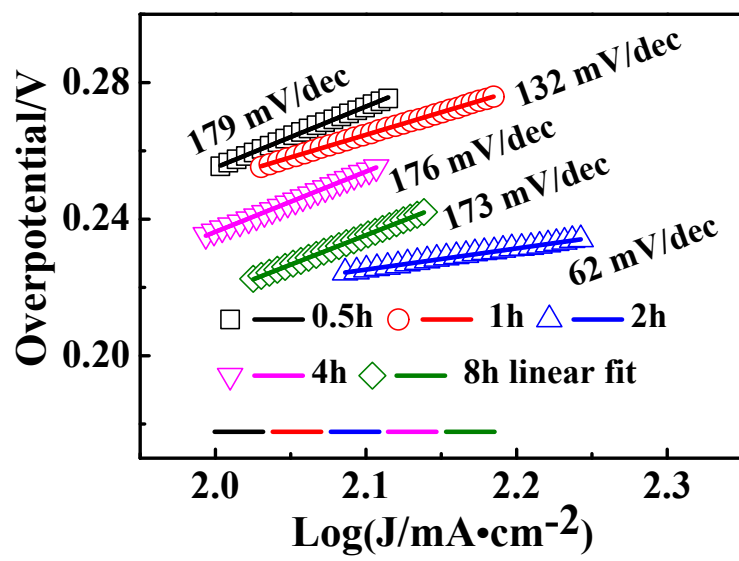


Figure S19 The influence of the reaction time on the tafel performance of (Ni,Fe)SO(OH)/NF electrode

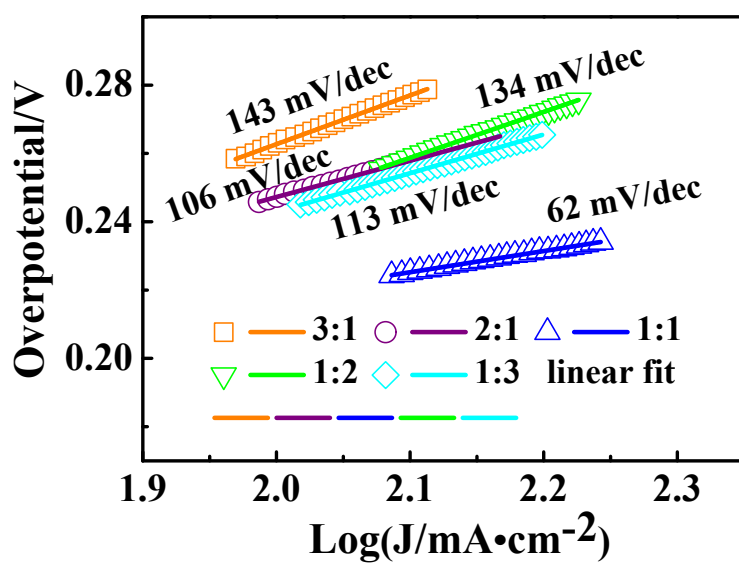


Figure S20 the influence of the ratio of m(Ni salt) and m(Fe salt) on the Tafel performance of

(Ni,Fe)SO(OH)/NF electrode

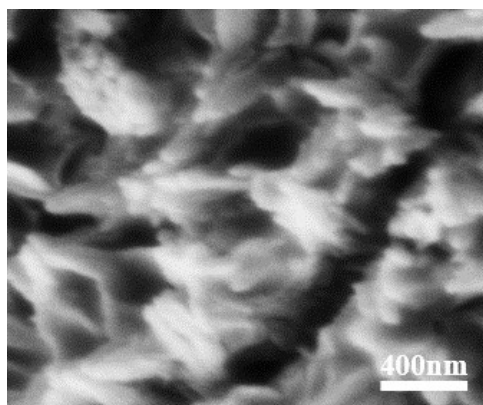


Figure S21 The morphology of (Ni, Fe)SO(OH) after OER stability test (1A/cm²,50h)

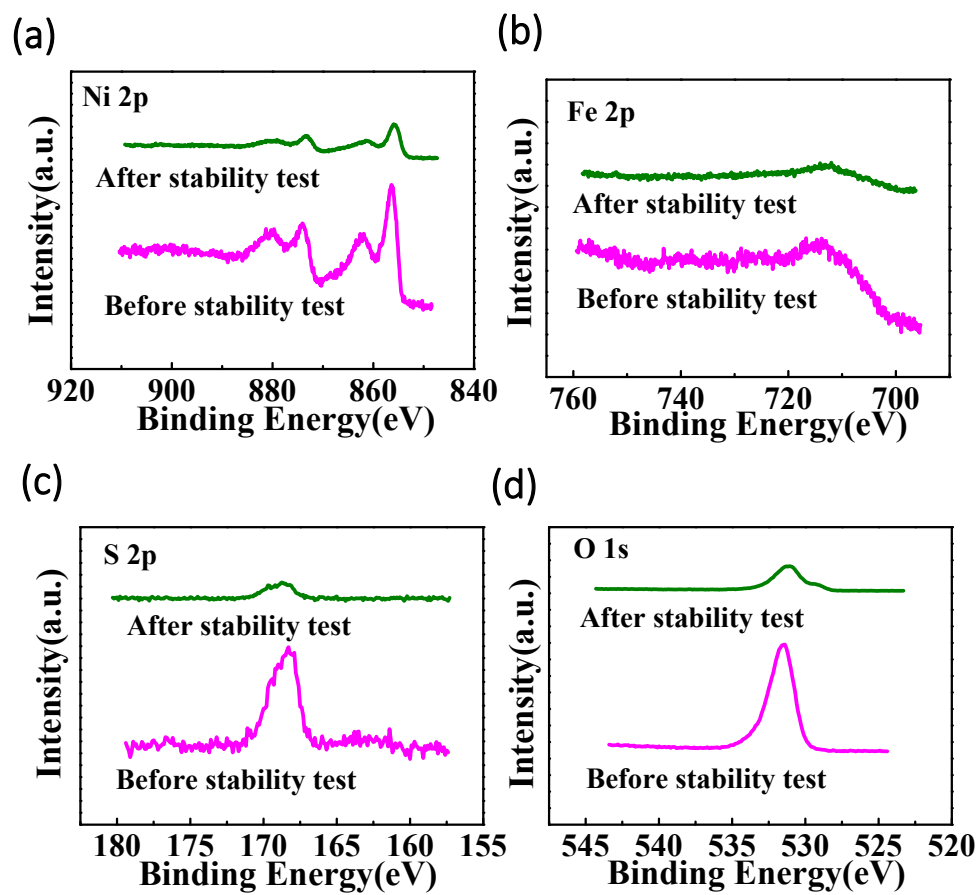


Figure S22 The XPS test of (Ni, Fe)SO(OH) after OER stability test (1A/cm², 50h)

Table S1. ICP test of electrolyte before and after OER stability test(1A/cm², 50h)

Electrolyte	Ni/ppm	Fe/ppm
Before OER stability test	ND	0.02
After OER stability test	0.02	0.03

Note: ND means “Not Detected”.

Supplementary METHODS

Calculation of electrochemically active surface area (*ECAS*)

The electrochemical double-layer capacitance C_{dl} is calculated according to the below equation:

$$C_{dl} = J_c \div v \quad (1)$$

The charge current J_c was derived from CV curves in the non-Faradaic capacitance current range. v is the scan rate as shown in **Fig S5**.

As shown in **Fig S7**, C_{dl} value of (Ni, Fe)SO(OH) is 23.31mF.

The electrochemically active surface area *ECAS* is calculated as the below equation according to the previous reports:

$$ECAS = C_{dl} \div C_s \quad (2)$$

According to the literatures, the specific capacitance value of the sample C_s is 0.040 mF/cm², so the *ECAS* of (Ni, Fe)SO(OH)/NF electrode is 582.5cm².

Table S2. The comparison of ECAS with the as-reported large-current-density OER catalysts.

Catalyst	ECAS(cm ² / cm ² GSA	Ref
(Ni, Fe)SO(OH)	582.5	This work
Fe-CoP/NF	485.75	<i>Adv. Sci.</i> 2018, 5, 1800949
Fe ₂ O ₃ @Ni ₂ P/Ni(PO ₃) ₂	527.5	<i>J. Mater. Chem. A</i> , 2019, 7, 965
Co ₃ O ₄ /Fe _{0.33} Co _{0.66} P	217.25	<i>Adv. Mater.</i> 2018, 30, 1803551
O-NFSECT	27.5	<i>Adv. Sci.</i> 2017, 4, 1600343
Fe(PO ₃) ₂	300	<i>PNAS</i> ,2017,114,5607
(Ni, Fe)OOH	147.5	<i>Energy Environ. Sci.</i> , 2018,11, 2858
Ni-Fe-OH@Ni ₃ S ₂ /NF	206	<i>Adv. Mater.</i> 2017, 29, 1700404

Table S3. Summary of as-reported large-current-density OER catalysts in 1M KOH electrolyte

Catalyst	j [A /cm ²]	overpoten tial (mV @ j)	Substrate	Ref
(Ni, Fe)SO(OH)	1	260	NF	This work
Fe-CoP/NF	1	428	NF	<i>Adv. Sci.</i> 2018, 5, 1800949
Fe ₂ O ₃ @Ni ₂ P/Ni(PO ₃) ₂	1	370	NF	<i>J. Mater. Chem. A</i> , 2019, 7, 965
Co ₃ O ₄ /Fe _{0.33} Co _{0.66} P	0.8	291	NF	<i>Adv. Mater.</i> 2018, 30, 1803551
O-NFSECT	1	305	Au-Ti plate	<i>Adv. Sci.</i> 2017, 4, 1600343
Fe(PO ₃) ₂	1	290	NF	<i>PNAS</i> , 2017, 114, 5607
(Ni, Fe)OOH	1	289	NF	<i>Energy Environ. Sci.</i> , 2018, 11, 2858
Ni-Fe-OH@Ni ₃ S ₂ /NF	0.8	548	NF	<i>Adv. Mater.</i> 2017, 29, 1700404

REFERENCES

1. L.-M. Cao, Y.-W. Hu, S.-F. Tang, A. Iljin, J. -W. Wang, Z. -M. Zhang and T. -Bu. Lu, *Adv. Sci.* 2018, **5**, 1800949.
2. X. Cheng, Z. Pan, C. Lei, Y. Jin, B. Yang, Z. Li, X. Zhang, L. Lei, C. Yuan and Y. Hou, *J. Mater. Chem. A*, 2019, **7**, 965.
3. X. Zhang, J. Li, Y. Yang, S. Zhang, H. Zhu, X. Zhu, H. Xing, Y. Zhang, B. Huang, S. Guo and E. Wang, *Adv. Mater.* 2018, **30**, 1803551.
4. J. Zhang, Y. Hu, D. Liu, Y. Yu and B. Zhang, *Adv. Sci.* 2017, **4**, 1600343.
5. H. Zhou, F. Yu, J. Sun, R. He, S. Chen, C. -W. Chu and Z. Ren, *PNAS*, 2017, **114**, 5607.
6. H. Zhou, F. Yu, Q. Zhu, J. Sun, F. Qin, L. Yu, J. Bao, Y. Yu, S. Chen and Z. Ren, *Energy Environ. Sci.*, 2018, **11**, 2858.
7. X. Zou, Y. Liu, G. -D. Li, Y. Wu, D. -P. Liu, W. Li, H. -W. Li, D. Wang, Y. Zhang and X. Zou, *Adv. Mater.* 2017, **29**, 1700404.